Scientific Research Publishing

Energy and Power Engineering, 2022, 14, 523-540
https://www.scirp.org/journal/epe
ISSN Online: 1947-3818
ISSN Print: 1949-243X

Analysis and Comparison of Doping Level Effects on a Crystalline Silicon PV Cell under Both Moderate Light Concentration and Normal Illumination Modes

Mahamadi Savadogo[1*], Adama Ouedraogo[1,2], Boubacar Soro[1,3], Zi Daouda Koudougou[1], Martial Zoungrana[1], Issa Zerbo[1]

[1]Laboratory of Thermal and Renewable Energies, Department of Physics, Unit of Training and Research in Pure and Applied Sciences, University Joseph Ki-Zerbo, Ouagadougou, Burkina Faso
[2]Centre Universitaire Polytechnique de Kaya (CUP-Kaya), Kaya, Burkina Faso
[3]Institut des Sciences et Technologies, Ouagadougou, Burkina Faso
Email: *savadogo.mahamadi1976@gmail.com

How to cite this paper: Savadogo, M., Ouedraogo, A., Soro, B., Koudougou, Z.D., Zoungrana, M. and Zerbo, I. (2022) Analysis and Comparison of Doping Level Effects on a Crystalline Silicon PV Cell under Both Moderate Light Concentration and Normal Illumination Modes. *Energy and Power Engineering*, **14**, 523-540.
https://doi.org/10.4236/epe.2022.1410028

Received: August 27, 2022
Accepted: October 14, 2022
Published: October 17, 2022

Copyright © 2022 by author(s) and Scientific Research Publishing Inc.
This work is licensed under the Creative Commons Attribution International License (CC BY 4.0).
http://creativecommons.org/licenses/by/4.0/

Open Access

Abstract

The main purpose of this work is to study doping level effects on a silicon PV cell under both moderate light concentration and normal illumination. This study also aims to compare the doping level effects under the both illumination modes. The results show for both illumination modes that diffusion parameters decrease with increasing doping level. These results are in agreement with the studies of the current and the voltage which showed for the two illumination modes that doping level increase leads to a decrease in current density and an increase in voltage. It also emerges for the two illumination modes and for the doping range 10^{13} cm^{-3} - 10^{16} cm^{-3}, a decrease of maximum power and conversion efficiency. The results also show that decrease of diffusion parameters is faster under moderate concentration in comparison with normal illumination. These results predict a greater variation rate of the current, the voltage, the maximum power and the conversion efficiency under moderate concentration compared to normal illumination. Contrary to diffusion parameters study, the results show higher variation rates of parameters under normal illumination. This is explained by the fact that under moderate concentration, carriers density is close to doping level: the cell is then in high injection condition. Consequently, under moderate concentration, carriers density is less sensitive to doping level variations. The study confirms that carriers density variation with the doping level is weak under the moderate concentration compared to normal illumination.

Keywords

Moderate Light Concentration, Doping Level, High Injection, Diffusion Parameters, Conversion Efficiency

1. Introduction

Photovoltaic solar energy is one of the most efficient solutions in the energy transition process. This rapid progress is due to the diversification of photovoltaic sectors, including that of high efficiency for light concentration [1]. The PV cell is submitted to increasing light concentration and achieves its performance improvement.

Schachtner *et al.* [2] working on a four-junction solar cell obtained a conversion efficiency of 44.5% for a light concentration of $C = 312$ Suns. In the same order, Dimroth *et al.* [3] found a conversion efficiency of 44.7% under concentration $C = 297$ Suns with a four-junction cell of GaInP/GaAs/GaInAsP/GaInAs type. And with the same type of PV cell, works of Tibbits *et al.* [4] led to a record conversion efficiency of 46.5% under a concentration of $C = 324$ Suns.

Under same illumination conditions, crystalline silicon solar cell presents a significantly lower conversion efficiency compared to previous PV cells [1] [5] [6]. Campbell *et al.* [7] showed that the upper bound on the efficiency of a concentrating silicon solar cell is 36% - 37% under AM 1.5 standard conditions. However, silicon wide availability and multi-junction cell relatively higher cost, make silicon a very promising technology for photovoltaics large-scale adoption [1].

Otherwise, several authors have worked on the influence of the doping level on the parameters of a crystalline silicon solar cell [8]-[16]. And these works showed that the diffusion parameters, the current density, the series resistance and the shunt resistance decrease with the doping level increasing. These works also showed the voltage increase with the doping level increase. However, these studies were carried out under normal illumination and non-concentrated.

Other authors such as Liou *et al.* [17] have carried out this study of doping level influence under concentrated illumination. However, in their study, the solar cell is under monochromatic illumination.

The main objective of this work is to study under moderate light concentration (C = 50 Suns) and under normal light illumination ($C = 1$ Sun), the cell's performances evolution with doping level. Due to silicon availability, this study is carried out with a crystalline silicon PV cell. And taking into account the real illumination conditions, the incident light is assumed to be multispectral. We also compare the doping level effect under moderate light concentration ($C = 50$ Suns) with its effect under normal illumination ($C = 1$ Suns). The PV cell is submitted respectively to a moderate concentration ($C = 50$ Suns) and to a normal illumination ($C = 1$ Sun). We then study for each illumination mode, the in-

fluence of doping level on photovoltaic parameters.

2. Methods and Theories

2.1. Excess Minority Carriers Density

The n^+-p-p^+ structure of the PV cell is assumed. This study is carried out in the quasi-neutral base (QNB) assumption [18] [19] which assumes that intrinsic electric field in the cell's base is neglected. First, the PV cell is submitted to a moderate light concentration (C = 50 Suns) as showed by Figure 1 and then to a normal light illumination (C = 1 Sun).

The continuity equation of minority charge carriers in steady state is given by:

$$\frac{\partial^2 \delta^\beta \left(x, N_b\right)}{\partial x^2} - \frac{\delta^\beta \left(x, N_b\right)}{\left(L^\beta \left(N_b\right)\right)^2} = -\frac{G^\beta \left(x\right)}{D^\beta \left(N_b\right)} \tag{1}$$

In Equation (1), $\delta^\beta (x, N_b)$ represents the excess minority carrier density which is a function of the both position x in the base and doping level N_b. $D^\beta (N_b)$ and $L^\beta (N_b)$ respectively represent the diffusion coefficient and the diffusion lenght. $G^\beta (x)$ is the carrier generation rate at the base deph x. The index β is linked to the illumination mode. So, under moderate light illumination C = 50 Suns and β = *con*. And under normal illumination mode C = 1 Sun and β = *nor*.

- Under moderate concentration (C = 50 Suns and β = *con*)

We take into account the electric field of electrons concentration gradient given by Equation (2) below [5] [6] [18]:

$$E\left(x\right) = \frac{D_p - D_n}{\mu_n + \mu_p} \cdot \frac{1}{\delta^{con}\left(x\right)} \cdot \frac{\partial \delta^{con}\left(x\right)}{\partial x} \tag{2}$$

The diffusion coefficient is given by Equation (3):

$$D^{con}\left(N_b\right) = \frac{\mu_n \left(N_b\right)\left[2D_n \left(N_b\right) - D_p\right] + \mu_p D_n \left(N_b\right)}{\mu_n \left(N_b\right) + \mu_p} \tag{3}$$

In Equation (3), $D_n (N_b)$ And D_p Respectively represent diffusion coefficients of electrons and holes. $\mu_n (N_b)$ and μ_p respectively represent mobility coefficients of electrons and holes.

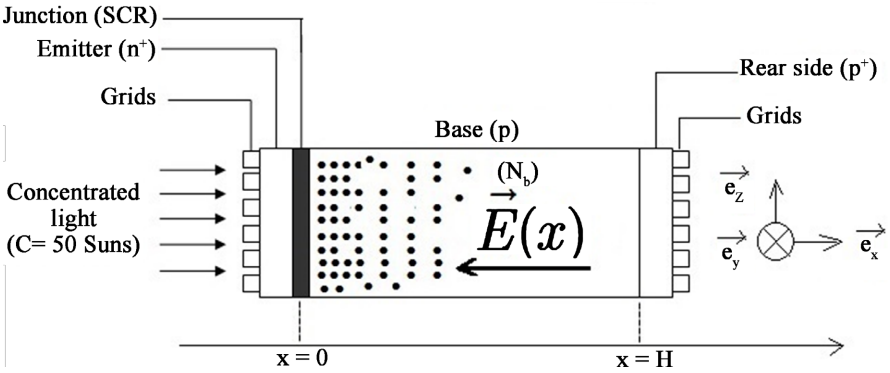

Figure 1. PV cell under moderated illumination concentration.

Equation (3) shows that under moderate concentration (C = 50 Suns), carriers diffusion depends on diffusion and mobility coefficients of electrons and holes.

The carrier generation rate $G^{con}(x)$ at the base depth x is given by [5] [6] [18] [20]:

$$G(x) = C \cdot \sum_{i=1}^{3} a_i e^{-b_i x} \tag{4}$$

- Under normal illumination mode (C = 1 Sun and $\beta = nor$)

The electric field of electrons concentration gradient is no longer taken into account. The diffusion coefficient in the base is then reduces to that of the electrons.

$$D^{nor}(N_b) = D_n(N_b) \tag{5}$$

The electron generation rate becomes:

$$G^{nor}(x) = \sum_{i=1}^{3} a_i e^{-b_i x} \tag{6}$$

As shown by Equations (7) to (9) below, electrons diffusion coefficient $D_n(N_b)$, their mobility coefficient $\mu_n(N_b)$ and their lifetime $\tau(N_b)$ depend on doping level (N_b) [17].

$$D_n(N_b) = \frac{1350 \cdot V_T}{\sqrt{1 + \frac{81 \cdot N_b}{N_b + 3,2.10^8}}} \tag{7}$$

$$\mu_n(N_b) = \frac{q}{kT} \cdot D_n(N_b) \tag{8}$$

$$\tau(N_b) = \frac{12}{1 + \frac{N_b}{5 \times 10^{16}}} (\mu s) \tag{9}$$

Then, whatever the illumination mode the diffusion coefficient in the base $D^{\beta}(N_b)$ is a function of doping level (N_b) as well as carriers the diffusion length $L^{\beta}(N_b)$ given by:

$$L^{\beta}(N_b) = \sqrt{D^{\beta}(N_b)\tau(N_b)} \tag{10}$$

By solving the continuity Equation (1), excess minority carriers density is determined by:

$$\delta^{\beta}(x, N_b) = A^{\beta} ch\left(\alpha^{\beta}(N_b)x\right) + B^{\beta} sh\left(\alpha^{\beta}(N_b)x\right) + \sum_{i=1}^{3} K_i^{\beta} \cdot e^{-b_i x} \tag{11}$$

Coefficients A^{β} and B^{β} are determined by using following boundary conditions [5] [6] [18] [20]:

- at the junction ($x = 0$)

$$D^{\beta}(N_b) \cdot \left.\frac{\partial \delta^{\beta}(x, N_b)}{\partial x}\right|_{x=0} = Sf \cdot \delta^{\beta}(x = 0, N_b) \tag{12}$$

Sf represents the junction dynamic velocity and is the sum of two contribu-

tions:

$$Sf = Sf_0 + Sf_j \tag{13}$$

Sf_0 is the junction intrinsic recombination velocity and is related to carriers losses at the junction. Sf_j is the junction dynamic velocity and defines the carriers flow imposed by an external load.

Thus, near the open circuit, the carriers flow through the junction is practically null and therefore $Sf_j \approx 0$ and $Sf \approx Sf_0$. In the short-circuit situation, the carriers flow through the junction is very important and therefore $Sf_j \to +\infty$ and $Sf \to +\infty$.

- at the cell's back ($x = H$)

$$D^{\beta}\left(N_b\right)\cdot\left.\frac{\partial\delta^{\beta}\left(x,N_b\right)}{\partial x}\right|_{x=H} = -S_b\cdot\delta^{\beta}\left(x=H,N_b\right) \tag{14}$$

S_b corresponds to the back surface recombination velocity and quantifies carriers losses at the PV cell rear side.

The ratio of doping level by carriers density is given by the following Equation (15).

$$Q^{\beta}\left(x,N_b\right) = \frac{N_b}{\delta^{\beta}\left(x,N_b\right)} \tag{15}$$

This ratio allows to compare carriers density evolution versus the doping level.

2.2. Determination of Electric Parameters

- **The current density**

The current density given by Equation (16) Is Found By Applying The Fick second law [5] [6] [18] [20] [21]:

$$J_{ph}^{\beta}\left(Sf,N_b\right) = q\cdot D^{\beta}\left(N_b\right)\cdot\left.\frac{\partial\delta^{\beta}\left(x,Sf,N_b\right)}{\partial x}\right|_{x=0} \tag{16}$$

The short-circuit current density is then defined by:

$$J_{sc}^{\beta} = \lim_{Sf\to+\infty} J_{ph}^{\beta} \tag{17}$$

- **The photo-voltage**

Using Boltzmann relation, we determine the expression of the voltage across the junction, given by Equation (18) [5] [6] [18] [20] [21]:

$$V_{ph}^{\beta}\left(Sf,N_b\right) = V_T\ln\left[\frac{\delta^{\beta}\left(x=0,Sf,N_b\right)}{n_0}+1\right] \tag{18}$$

Then the cell's open-circuit voltage is given by:

$$V_{oc}^{\beta} = \lim_{Sf\to 0} V_{ph}^{\beta} \tag{19}$$

V_T represents the thermal voltage and is given by $V_T = kT/q$, n_0 represents electrons density in thermodynamic equilibrium and is given by $n_0 = (n_i)^2/N_b$. At $T = 300$ K, the both electrons intrinsic concentration n_i and the silicon energy

gap $Eg(T)$ are calculated by following Equations (20) and (21) [6]:

$$n_i = A_n \cdot T^{\frac{3}{2}} \cdot \exp\left(-\frac{Eg(T)}{2kT}\right) \tag{20}$$

$$Eg(T) = 1.1557 - \frac{7.021\times10^{-4}T^2}{T+1108} \tag{21}$$

A_n represents the materiel specific constant. For the silicon A_n = 3.87 × 10^{16} and k the Boltzmann constant.

The electric power

The electric power delivered by the PV cell is given by Equation (22) below [5] [6] [20] [21]:

$$P^{\beta}(Sf, N_b) = V_{ph}^{\beta}(Sf, N_b) \cdot J_{ph}^{\beta}(Sf, N_b) \tag{22}$$

- **The conversion efficiency**

The solar cell's conversion efficiency is calculated by using the following Equation (23) [5] [6] [20]:

$$\eta^{\beta}(N_b) = \frac{(P^{\beta})_{\max}(Sf, N_b)}{P_{inc}} \tag{23}$$

$(P^{\beta})_{\max}$ is the maximum power at the illumination mode β and P_{inc} represents the power of the incident light under Air Mass 1.5 standard conditions.

2.3. Determination of Parameters Variation Rate

The variation rate of a parameter X is calculated as a percentage. It is defined by:

$$\left|\frac{X_f - X_i}{X_i}\right| \times 100 \tag{24}$$

where X_i and X_f represent respectively the initial and final values of X.

3. Results and Discussion

3.1. Doping Level Effect on Diffusion Parameters

Figure 2 and Figure 3 below give respectively variations of diffusion coefficient and diffusion length with doping level (N_b) increase, under moderate light concentration (C = 50 Suns) and normal light illumination mode (C = 1 Sun).

Figure 2 and Figure 3 show that for a given doping level (N_b), diffusion parameters are higher under moderate light concentration (C = 50 Suns) compared to the normal illumination mode (C = 1 Sun).

It also appears that whatever the illumination mode (C = 50 Suns or C = 1 Sun), the diffusion parameters decrease with the doping level increase. This decrease of the diffusion parameters results in a decrease of carriers flux through the junction. This allows predicting a decrease of the current density with the base doping level increase. The decrease of the diffusion parameters also results in carriers storage near the pn junction. This also allows us to predict an increase of the photo voltage with the base doping level increase.

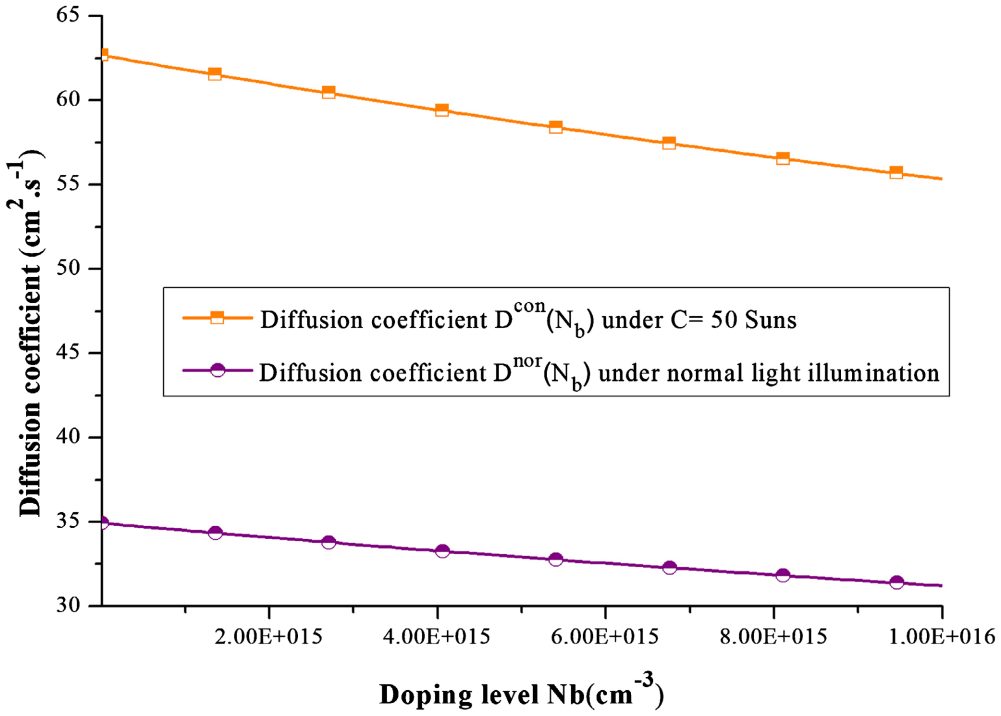

Figure 2. Diffusion coefficient variation versus doping level.

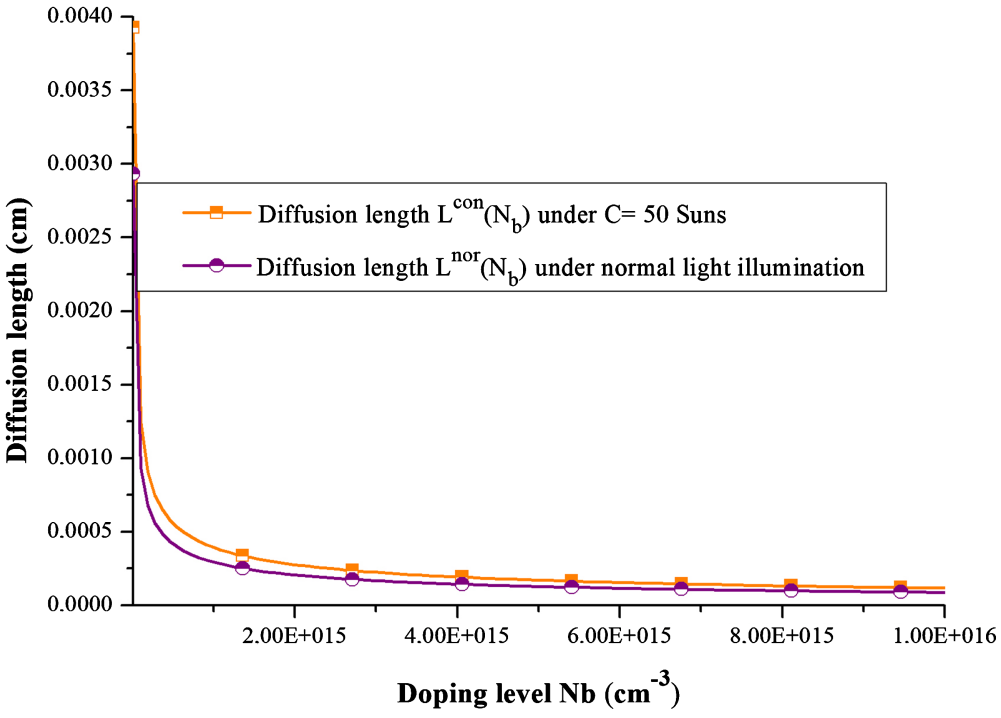

Figure 3. Diffusion length versus base doping level.

Table 1 gives respectively under moderate light concentration and normal light illumination, doping level values and corresponding diffusion parameters values as well as their variation rates.

Table 1 shows that under moderate light concentration (C = 50 Suns), doping

level increase from 10^{13} cm^{-3} to 10^{16} cm^{-3} leads to diffusion coefficient decrease from 62.68 $cm^2 \cdot s^{-1}$ to 55.34 $cm^2 \cdot s^{-1}$. This is equivalent to 11.71% decrease in the diffusion coefficient. At the same time, under normal light illumination the diffusion coefficient decreases from 34.93 $cm^2 \cdot s^{-1}$ to 31.21 $cm^2 \cdot s^{-1}$. That is equivalent to 10.65% decrease in the diffusion coefficient.

It also appears from Table 1 that under moderate light concentration, the diffusion length decreases by 97.00% while under normal light illumination it decreases by 96.98%.

These results show that doping level impact on diffusion parameters is more felt under the moderate light concentration mode compared to normal light illumination.

3.2. Doping Level Effect on Photo-Current Density

The current density profile is plotted under a moderate light concentration (C =

Table 1. Illumination modes, diffusion parameters under different doping level and their variation rates.

N_b (cm^{-3})	Moderate light concentration (C = 50 Suns)		Normale light illumination (C = 1 Sun)	
	D^{con} ($cm^2 \cdot s^{-1}$)	L^{con} (cm)	D^{nor} ($cm^2 \cdot s^{-1}$)	L^{nor} (cm)
10^{13}	62.68	3.93×10^{-3}	34.93	2.93×10^{-3}
10^{16}	55.34	1.18×10^{-4}	31.21	8.86×10^{-5}
Variation rate (%)	11.71	97.00	10.65	96.98

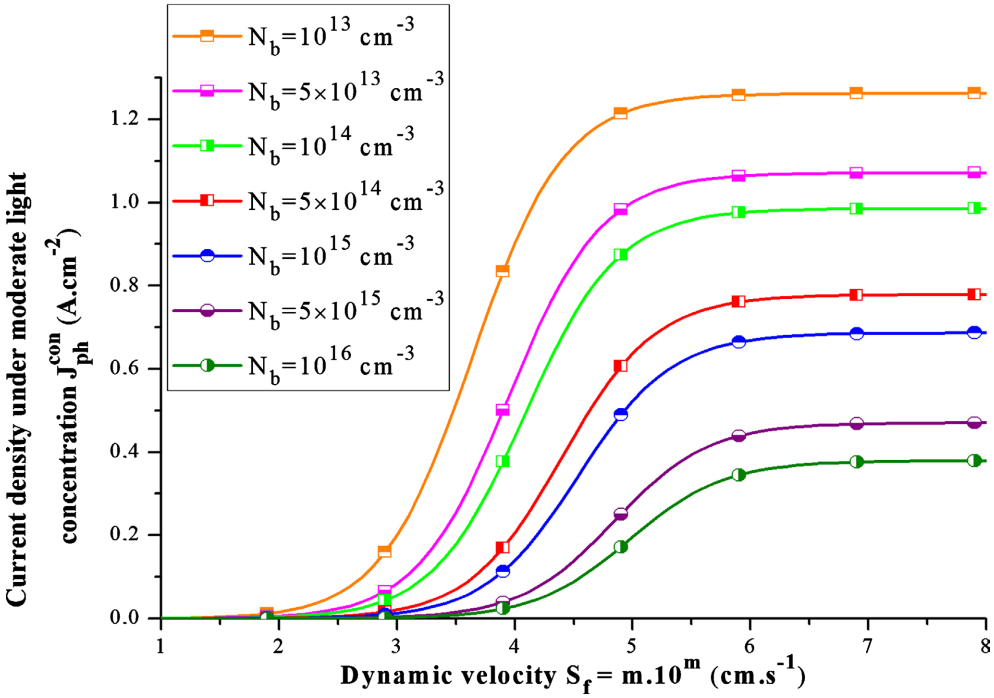

Figure 4. Current density profile versus dynamic velocity under moderate light concentration and for different doping level.

50 Suns) for different doping level as showed by the following Figure 4.

Figure 4 shows that for a given doping level, the current density is null near the open circuit where the dynamic velocity $Sf \approx 0$. The current density then increases with the dynamic velocity to reach its maximum in the short-circuit situation ($Sf \to +\infty$).

Figure 4 also shows that doping level increasing leads to current density decrease. This result agrees with the study of doping level influence on diffusion parameters carried out above. Indeed, this study had predicted a decrease in current density with doping level increase. These results are also consistent with those of Ould Cheikh *et al.* [14] and Samoura *et al.* [15] who worked under normal illumination.

Table 2 gives for the two illumination modes and for different doping level, the short-circuit current as well as its variation rate.

Table 2 shows that under moderate light concentration (C = 50 Suns), the short-circuit current density decreases from 1262.82 mA·cm^{-2} to 379.36 mA·cm^{-2}, when the doping level increases from 10^{13} cm^{-3} to 10^{16} cm^{-3}. This is equivalent to 69.96% decrease in short-circuit current density.

At the same time, under normal ligh illumination, the current density decreases from 23.88 mA·cm^{-2} to 6.32 mA·cm^{-2}. This is equivalent to 73.53% decrease in short-circuit current density.

These results show that doping concentration effect on short-circuit current density is greater under normal illumination compared to moderate illumination mode. These results are in contradiction with diffusion parameters study. Indeed, this study had shown a greater effect of the doping level under moderate concentration compared to the normal illumination mode. This contradictory result is linked to the fact that under moderate light concentration carriers generation is strong. The carriers density is very high and close to doping level and consequently less sensitive to the doping rate variations. The PV cell is then said

Table 2. Illumination modes, short-circuit current density for different doping levels and its variation rates.

doping level N_b (cm^{-3})	Short-circuit current density (mA·cm^{-2}) under moderate concentration (C = 50 Suns)	Short-circuit current density (mA·cm^{-2}) under normal illumination (C = 1 Sun)
10^{13}	1262.82	23.88
5×10^{13}	1071.83	19.99
10^{14}	985.89	18.24
5×10^{14}	778.86	14.04
10^{15}	686.83	12.20
5×10^{15}	470.49	7.99
10^{16}	379.36	6.32
Variation rate (%)	69.96	73.53

to be in high injection condition [18] [22].

3.3. Doping Level Effect on the Photo Voltage

As show by following Figure 5, the PV cell's voltage profile versus dynamic velocity was also plotted for different doping level (N_b) and under moderate light concentration.

For a given doping level, Figure 5 shows that near the open-circuit the voltage is maximum and constant. It then decreases with the dynamic velocity and becomes null in short-circuit situation.

It also emerges from Figure 5 that the doping level increase leads to photo voltage increase. This result also is also agrees with diffusion parameters study which had predicted an increase in voltage with doping level increase. Working under non-concentrated illumination Ould Cheikh *et al.* [14] and Trukhanov *et al.* [16] also found similar results.

The following Table 3 gives for the two illumination modes and for different doping levels, the open-circuit voltage as well as its variation rate.

Table 3 shows that under moderate light concentration, the open-circuit voltage increases from 995.74 mV to 1055.89 mV when the doping level increases from 10^{13} cm^{-3} to 10^{16} cm^{-3}. This is equivalent to 6.04% increase in open-circuit voltage.

At the same time, under normal illumination mode the open-circuit voltage increases from 900.63 mV to 957.32 mV. This is equivalent to 6.29% increase in open-circuit voltage.

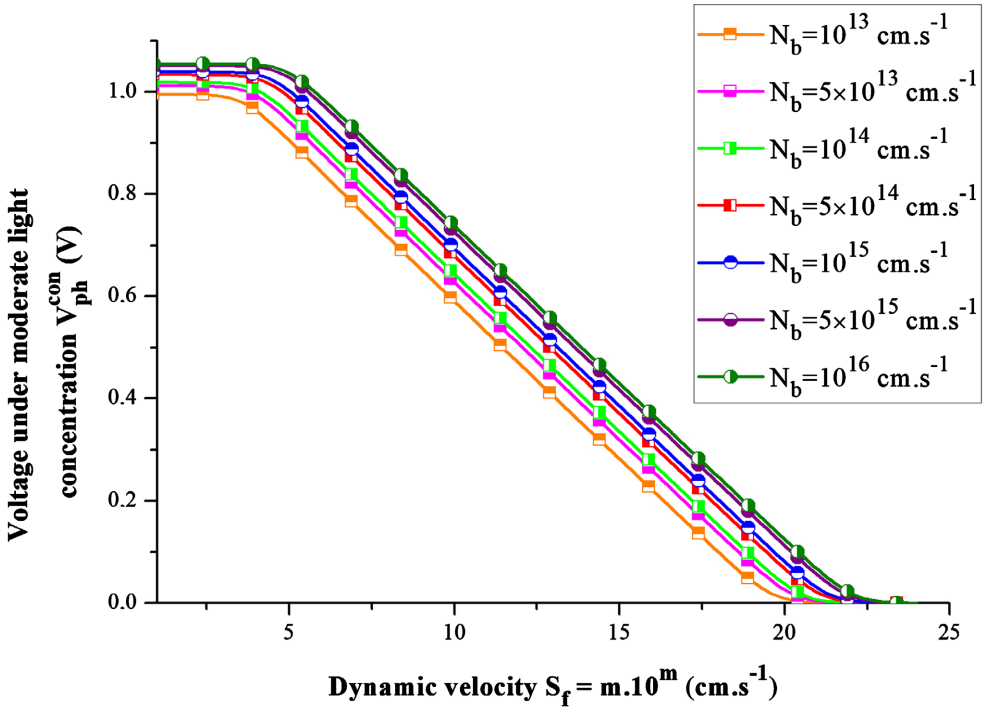

Figure 5. PV cell voltage profile versus dynamic velocity under moderate concentration and for different doping level.

Table 3. Illumination modes, open-circuit voltage for different doping level and its variation rate.

doping level N_b (cm^{-3})	Open-circuit voltage (mV) under moderate illumination (C = 50 Suns)	Open-circuit voltage (mV) under normal illumination (C = 1 Sun)
10^{13}	995.74	900.63
5×10^{13}	1012.56	917.09
10^{14}	1019.40	923.72
5×10^{14}	1034.22	937.86
10^{15}	1040.02	943.27
5×10^{15}	1051.73	953.77
10^{16}	1055.89	957.32
Variation rate (%)	6.04	6.29

This result shows that the doping level effect on the open-circuit voltage is also greater for the normal illumination mode compared to the moderate light concentration.

This is in contradiction with the diffusion parameters study carried out earlier in this article. But is explained by importance of carriers density under moderate light concentration. The carriers density is close to the doping level and less sensitive to variations in this doping level. This implies open-circuit voltage low variation under moderate light concentration compared to normal illumination mode.

3.4. Doping Level Effect on the Electric Power

The electric power profile is plotted under moderate light concentration and for different values of the doping level (N_b) as shows by following **Figure 6**.

For a given doping level, **Figure 6** shows that the electric power increases with the dynamic velocity to reach it maximum before decreases. The electric power is null near open-circuit and in short-circuit situation. **Figure 6** also shows that the maximum power decreases when the doping level increases from 10^{13} cm^{-3} to 10^{16} cm^{-3}.

Table 4 gives for the two illumination modes, the maximum power for different doping level and its variation rate.

Under moderate light concentration the maximum power decreases from 1108.50 mW·cm^{-2} to 355.22 mW·cm^{-2} when the doping level increases from 10^{13} cm^{-3} to 10^{16} cm^{-3}. This is equivalent to 67.95% decrease in the maximum power. At the same time under normal illumination mode the maximum power decreases from 18.76 mW·cm^{-2} to 5.31 mW·cm^{-2}. This corresponds to 71.70% decrease in the maximum power.

This result also shows that doping level effect on the maximum power is greater for normal illumination mode compared to moderate light concentration.

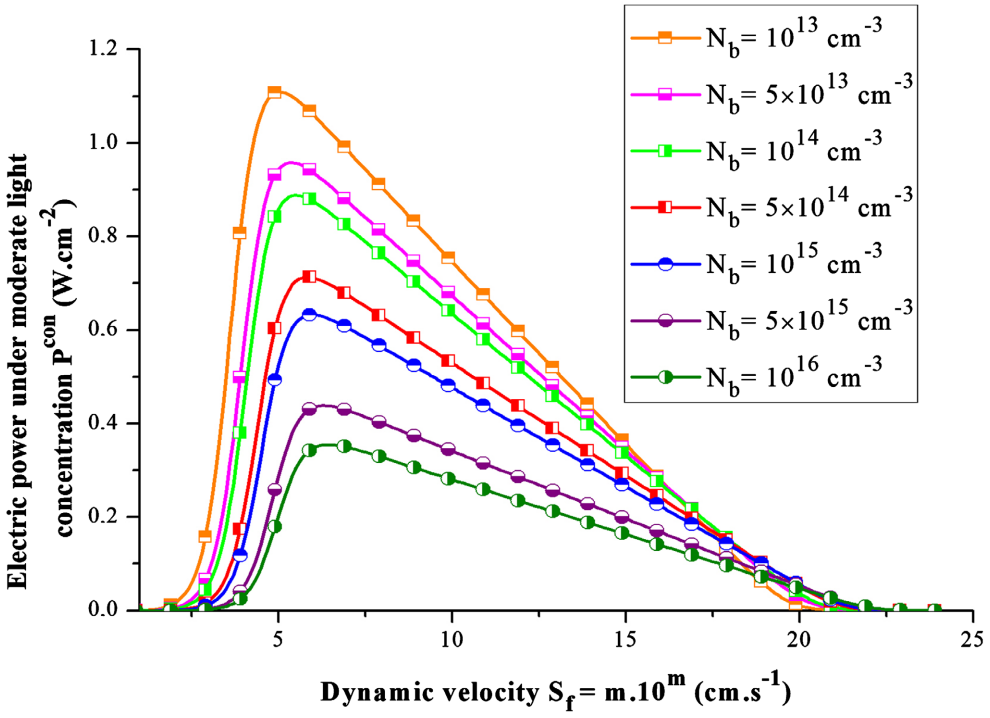

Figure 6. Electric power profile under moderate light concentration for different doping levels.

Table 4. Illumination modes, maximum power for different doping levels and its variation rate.

doping level N_b (cm^{-3})	Maximum power ($mW{\cdot}cm^{-2}$) under moderate concentration (C = 50 Suns)	Maximum power ($mW{\cdot}cm^{-2}$) under normal illumination (C = 1 Sun)
10^{13}	1108.50	18.76
5×10^{13}	958.45	16.02
10^{14}	888.22	14.74
5×10^{14}	712.83	11.54
10^{15}	632.56	10.09
5×10^{15}	438.69	6.69
10^{16}	355.22	5.31
Variation rate (%)	67.95	71.70

3.5. Doping Level Effect on Conversion Efficiency

Figure 7 below gives, for the two illumination modes, the variations of the conversion efficiency with the doping level.

Figure 7 shows that whatever the illumination mode, the conversion efficiency decreases when the doping level increases.

The following Table 5 gives under moderate light concentration and under normal illumination, the conversion efficiency for different doping level and its variation rate.

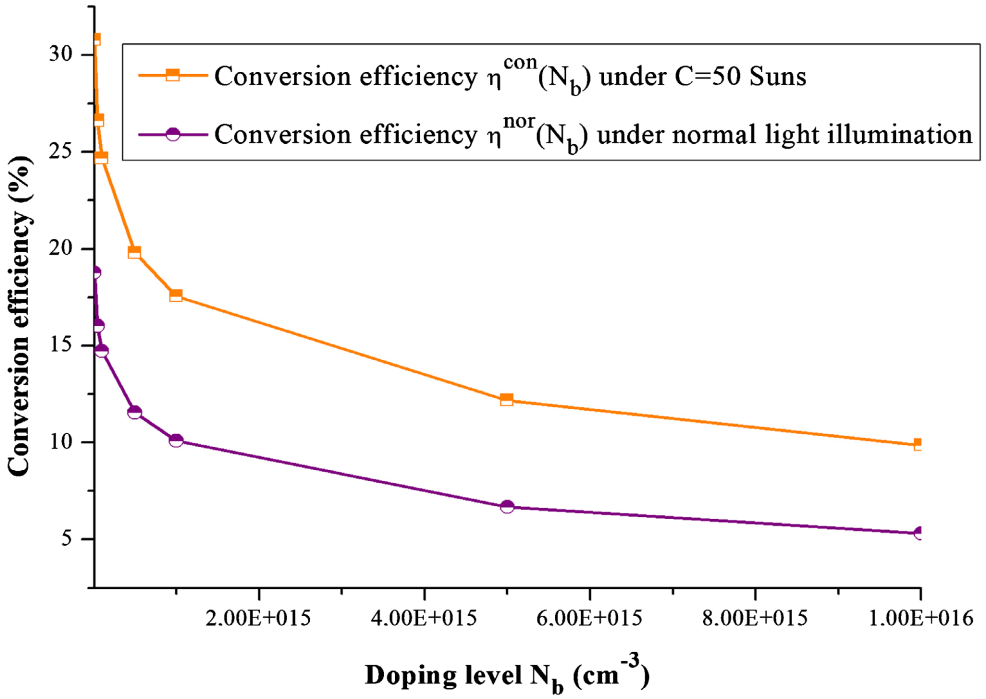

Figure 7. Conversion efficiency versus doping level.

Table 5. Illumination modes, conversion efficiency for different doping level and its variation rate.

doping level N_b (cm^{-3})	Conversion efficiency (%) under moderate concentration (C = 50 Suns)	Conversion efficiency (%) under normal illumination (C = 1 Sun)
10^{13}	30.79	18.76
5×10^{13}	26.62	16.02
10^{14}	24.67	14.74
5×10^{14}	19.80	11.54
10^{15}	17.57	10.09
5×10^{15}	12.18	6.69
10^{16}	9.87	5.31
Variation rate (%)	67.94	71.70

Table 5 shows that under moderate light concentration, the conversion efficiency decreases from 30.79% to 9.87% with a variation rate of 67.94%. Under normal illumination, the conversion efficiency decreases from 18.76% to 5.31% with a variation rate of 71.70%. These results show a significant effect of doping level under normal illumination mode compared to moderate light concentration mode.

As we have already explained, this fact is due to carriers density importance under moderate light concentration compared to normal illumination. Thus, under moderate light concentration, the carriers density is significant and close

to the doping level and therefore not very sensitive to variations in the doping level. However, under normal illumination, the carriers density is significantly lower and then more sensitive to variations in the doping level.

3.6. Comparison of Carrier Densities with the Doping Level

We plotted for the two illumination modes, the variations of the ratio of the doping level by the carriers density as show by **Figure 8**. The carriers density is calculated near the open-circuit operating point and at the base depth $x = 0.0001$ cm, very close to the junction.

Figure 8 shows that the quotient of doping level by carriers density increases very rapidly in normal illumination mode compared to moderate light concentration mode. This reflects the fact that under moderate light concentration, the carrier density is very close to the doping level.

Pelanchon *et al.* [18] also showed that under light concentration carriers density is close to doping level. This is due to carriers strong generation related to the illumination level. The cell then is in high injection condition [18] [23].

However, in normal illumination mode, the carrier density is very low compared to the doping rate.

As shown by **Figure 9**, the variations of the ratio of the doping level by carriers density were also plotted, in an intermediate operating point and for the two illumination modes at the same depth $x = 0.0001$ cm.

It emerges from **Figure 9** that the ratio of the doping level by carriers density also increases rapidly in normal illumination mode in comparison with the

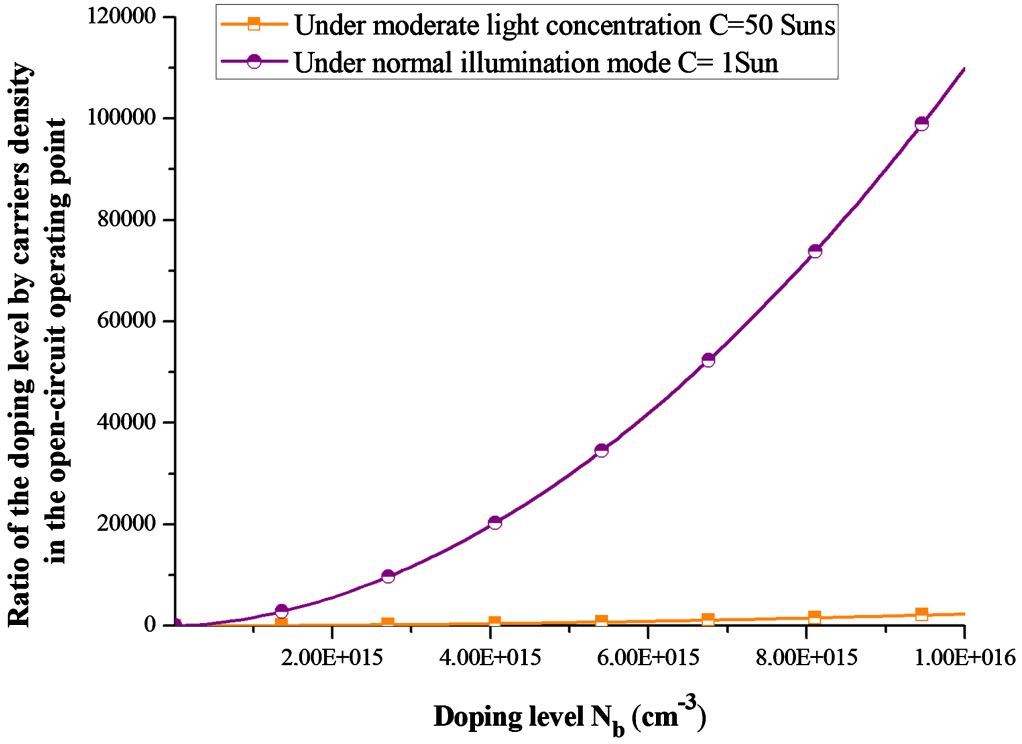

Figure 8. Carriers density variation in the open-circuit operating point.

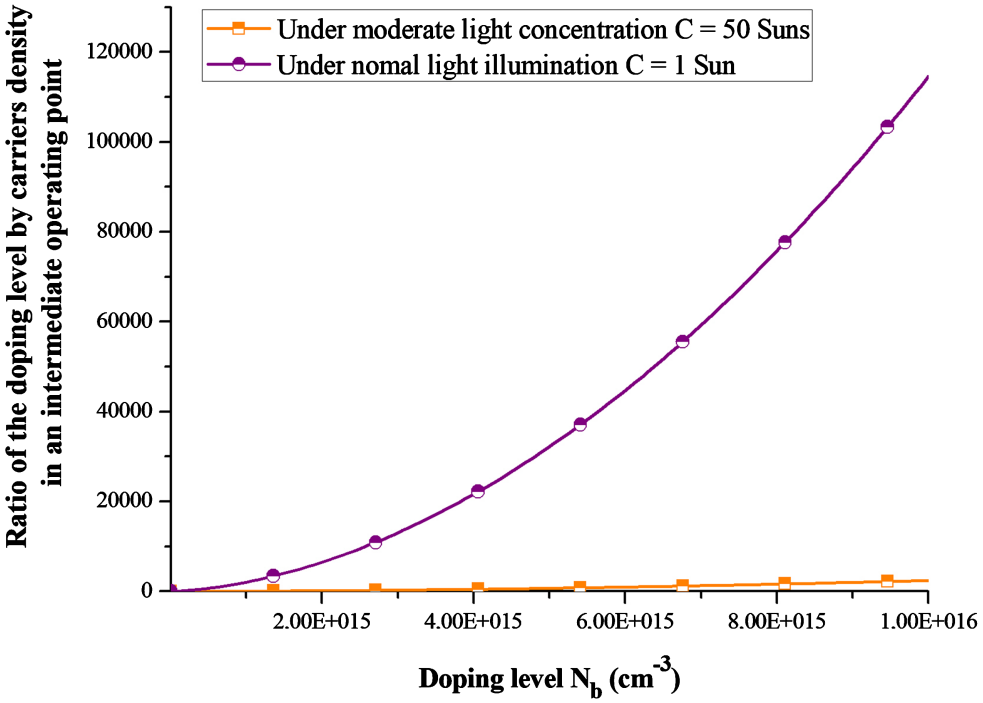

Figure 9. Carriers density variation in an intermediate operating point.

moderate concentration illumination mode. This result proves that in an intermediate operating point and under moderate light concentration, the doping level is close to carriers density. However, under normal illumination mode, carriers density is significantly low compared to the doping level.

Under the two illumination modes, the variations of the ratio of the doping level by carriers density were also plotted in the short-circuit situation as shown by **Figure 10** below.

The results also show that in the short-circuit situation and under moderate light concentration, carrier density is close to doping level. However under normal illumination mode, carriers density is low compared to the doping level. These facts result in a greater effect of doping rate on carriers density under normal illumination mode compared to the moderate light concentration mode.

4. Conclusions

An analysis of the doping level effect was carried out under moderate light concentration (C = 50 Suns) and under normal light illumination (C = 1 Sun).

It appears for the both illumination modes a decrease of the diffusion parameters, of the current density, of the maximum power and the conversion efficiency with the doping level increase while the photo-voltage increases.

The results also showed that diffusion parameters variation rate with the doping level is greater under moderate light concentration compared to the normal illumination mode.

However, results show that the short-circuit current, the open-circuit voltage, the maximum power and the conversion efficiency all present higher variation

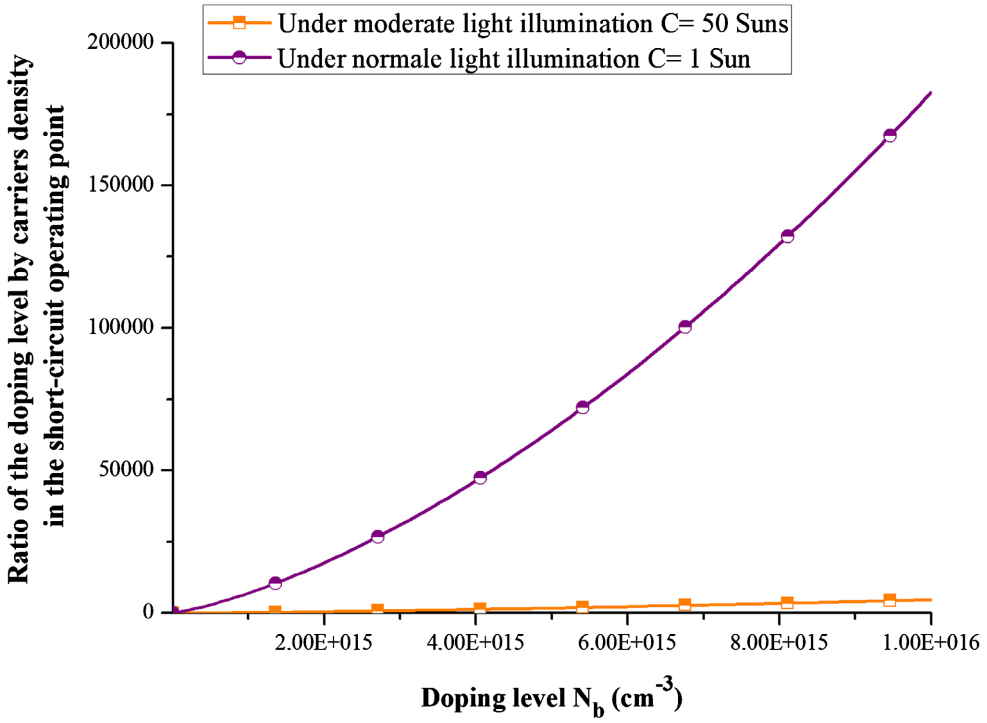

Figure 10. Carriers density variation in short-circuit operating point.

rates under normal illumination. This result is in contradiction with diffusion parameters study but can be explained by the fact that under moderate light concentration carriers strong generation leads to high carriers density values. The carriers density is very high and close to doping level and consequently less sensitive to the doping level variations: the PV cell is then in high injection condition. Carriers density study confirms that its variation with the doping level is weak under moderate light concentration compared to the normal illumination mode.

Acknowledgements

The authors wish to thank International Science Program (ISP) for funding our research group and allowing conducting this work.

Conflicts of Interest

The authors declare no conflicts of interest regarding the publication of this paper.

References

[1] El Chaar, L., lamont, L.A. and El Zein, N. (2011) Review of Photovoltaic Technologies. *Renewable and Sustainable Energy Reviews*, **15**, 2165-2175. https://doi.org/10.1016/j.rser.2011.01.004

[2] Schachtner, M., Prado, M.L., Reichmuth, S.K., Siefer, G. and Bett, A.W. (2016) Analysis of a Four Lamp Flash System for Calibrating Multi-Junction Solar Cells under Concentrated Light. *AIP Conference Proceedings*, **1679**, Article No. 050012.

https://doi.org/10.1063/1.4931533

[3] Dimroth, F., Grave, M., Beutel, P., Fiedeler, U., Karcher, C., Tibbits, T.N.D., Oliva, E., Siefer, G., Schachtner, M., Wekkeli, A., Bett, A.W., Krause, R., Piccin, M.T., Blanc, N., Drazek, C.T., Guiot, E., Ghyselen, B., Salvetat, T., Tauzin, A., Signamarcheix, T., Dobrich, A., Hannappel, T. and Schwarzburg, K. (2014) Wafer Bonded Four-Junction GaInP/GaAs//GaInAsP/GaInAs Concentrator Solar Cells with 44.7% Efficiency. *Progress in Photovoltaics*: *Research and Applications*, **22**, 277-282. https://doi.org/10.1002/pip.2475

[4] Tibbits, T.N.D., Beutel, P., Grave, M., Karcher, C., Oliva, E., Siefer, G., Wekkeli, A., Schachtner, M., Dimroth, F., Bett, A.W., Krause, R., Piccin, M., Blanc, N., Munoz-Rico, M., Arena, C., Guiot, E., Charles-Alfred, C., Drazek, C., Janin, F., Farrugia, L., Hoarau, B., Wasselin, J., Tauzin, A., Signamarcheix, T., Hannappel, T., Schwarzburg, K. and Dobrich, A. (2014) New Efficiency Frontiers with Wafer-Bonded Multi-Junction Solar Cells. 29*th European PV Solar Energy Conference and Exhibition*, Amsterdam, 22-26 September 2014, 1975-1978.

[5] Zoungrana, M., Zerbo, I., Savadogo, M., Tiedrebeogo, S., Soro, B. and Bathiebo, D.J. (2017) Effect of Light Intensity on the Performance of Silicon Solar Cell. *Global Journal of Pure and Applied Sciences*, **23**, 123-129. https://doi.org/10.4314/gjpas.v23i1.12

[6] Savadogo, M., Zoungrana, M., Zerbo, I., Soro, B. and Bathiebo, D.J. (2017) 3-D Modeling of Grains Sizes Effects on Polycrystalline Silicon Solar Cell under Intense Light Illumination. *Sylwan*, **161**, 2-13.

[7] Campbell, P. and Green, M.A. (1986) The Limiting Efficiency of Silicon Solar cells under Concentrated Sunlight. *IEEE Transactions on Electron Devices*, **33**, 234-239. https://doi.org/10.1109/T-ED.1986.22472

[8] Reis, I.E., Riepe, S., Koch, W., Bauer, J., Beljakowa, S., Breitenstein, O., Habenicht, H., Krener-Kiel, D., Pens, G., Schn, J. and Seifert, W. (2009) Effect of Impurities on Solar Cell Parameters in Intentionally Contaminated Multicrystalline Silicon. 24*th European Photovoltaic Solar Energy Conference*, Hamburg, 21-25 September 2009.

[9] Wegierek, P.A., Pastuszak, J., Dziadosz, K. and Turek, M. (2020) Influence of Substrate Type and Dose of Implantedions on the Electrical Parameters of Silicon in Terms of Improving the Efficiency of Photovoltaic Cells. *Energies*, **13**, Article No. 6708. https://doi.org/10.3390/en13246708

[10] Kolsi, S., Amar, M.B., Samet, H. and Ouali, A. (2012) Effect of Gaussian Doping Profile on the Performance of a Thin Film Polycrystalline Solar Cell. *EPJ Web of Conferences*, **29**, Article No. 00025. https://doi.org/10.1051/epjconf/20122900025

[11] Assa, B., Kivambe, M.M., Hossain, M.I., El Daif, O., Abdallah, A.A., Ali, F. and Tabet, N. (2015) Emerging Frontiers of N-Type Silicon Material for Photovoltaic Applications: The Impurity-Defect Interactions. *Frontiers in Nanoscience and Nanotechnology*, **1**, 2-12. https://doi.org/10.15761/FNN.1000102

[12] Geerligs, L.J. and Macdonald, D. (2004) Base Doping and Recombination Activity of Impurities in Crystalline Silicon Solar Cells. *Progress in Photovoltaics*: *Research and Applications*, **12**, 309-316. https://doi.org/10.1002/pip.546

[13] Sane, M. and Barro, F.I. (2015) Effect of both Magnetic Field and Doping Density on Series and Shunt Resistances under Frequency Modulation. *Indian Journal of Pure and Applied Physics*, **53**, 590-595.

[14] Ould Cheikh, M.L., Seibou, B., El Moujtaba, M.A.O., Faye, K., Wade, M. and Sissoko, G. (2015) Study of Base Doping Rate Effect on Parallel Vertical Junction Silicon Solar Cell under Magnetic Field. *International Journal of Engineering Trends and*

Technology, **19**, 44-55. https://doi.org/10.14445/22315381/IJETT-V19P210

[15] Samoura, A., Sakho, O., Faye, O. and Beye, A.C. (2017) Base Doping Effects on the Efficiency of Vertical Parallel Junction Solar Cells. *Open Journal of Applied Sciences*, **7**, 282-290. https://doi.org/10.4236/ojapps.2017.76023

[16] Trukhanov, V.A., Bruevich, V.V. and Paraschuk, D.Y. (2011) Effect of Doping on Performance of Organic Solar Cell. *Physical Review B*, **84**, Article ID: 205318. https://doi.org/10.1103/PhysRevB.84.205318

[17] Liou, J.J. and Wong, W.W. (1992) Comparison and Optimization of the Performance of Si and GaAs Solar Cells. *Solar Energy Materials and Solar Cells*, **28**, 9-28. https://doi.org/10.1016/0927-0248(92)90104-W

[18] Pelanchon, F., Sudre, C. and Moreau, Y. (1992) Solar Cells under Intense Light Concentration: Numerical and Analytical Approaches. 11*th European Photovoltaic Solar Energy Conference*, Montreux, 12-16 October 1992, 265-267.

[19] Fossum, J.G., Burgess, E.L. and Lindholm, F.A. (1978) Silicon Solar Cell Designs Based on Physical Behavior in Concentrated Sunlight. *Solid-State Electronics*, **21**, 729-737. https://doi.org/10.1016/0038-1101(78)90005-9

[20] Savadogo, M., Soro, B., Konate, R., Sourabie, I., Zoungrana, M., Zerbo, I. and Bathiebo, D.J. (2020) Temperature Effect on Light Concentration Silicon Solar Cell's Operating Point and Conversion Efficiency. *Smart Grid and Renewable Energy*, **11**, 61-72. https://doi.org/10.4236/sgre.2020.115005

[21] Savadogo, M., Konfe, A., Sourabie, I., Soro, B., Konate, R., Zoungrana, M., Zerbo, I. and Bathiebo, D.J. (2021) Light Concentration Solar Cell: Temperature Proper and Dynamic Effect on Electrical Parameters Determined by Using J-V and P-V Characteristics. *Global Journal of Pure and Applied Sciences*, **27**, 341-347. https://doi.org/10.4314/gjpas.v27i3.10

[22] Mialhe, P., Affour, B., El-Hajj, K. and Khoury, A. (2015) High Injection Effects on Solar Cell Performances. *Active and Passive Electronic Components*, **17**, 227-232. https://doi.org/10.1155/1995/93424

[23] Goradia, C. and Weinberg, I. (1985) Theory of the High Base Resistivity n^+pp^+ Silicon Solar Cell and Its Application to Radiation Damage Effects. *Journal of Applied Physics*, **57**, 4752-4760. https://doi.org/10.1063/1.335340